

COO-4246-8

MICROSTRUCTURAL EFFECTS IN ABRASIVE WEAR

Quarterly Progress Report
for the period 15 December 1978 - 15 March 1979

Nicholas F. Fiore, Thomas H. Kosel, William Konkel
and John Fulcher

Department of Metallurgical Engineering and Materials Science
Notre Dame, IN 46556

NOTICE

This report was prepared as an account of work sponsored by the United States Government. Neither the United States nor the United States Department of Energy, nor any of their employees, nor any of their contractors, subcontractors, or their employees, makes any warranty, express or implied, or assumes any legal liability or responsibility for the accuracy, completeness or usefulness of any information, apparatus, product or process disclosed, or represents that its use would not infringe privately owned rights.

NOTICE

This report was prepared as an account of work sponsored by the United States Government. Neither the United States nor the United States Department of Energy, nor any of their employees, nor any of their contractors, subcontractors, or their employees, makes any warranty, express or implied, or assumes any legal liability or responsibility for the accuracy, completeness, or usefulness of any information, apparatus, product or process disclosed or represents that its use would not infringe privately owned rights.

15 April 1979

Prepared for

U. S. Department of Energy

Under Contract No. EF-77-S-02-4246

fb
DISTRIBUTION OF THIS DOCUMENT IS UNLIMITED

DISCLAIMER

This report was prepared as an account of work sponsored by an agency of the United States Government. Neither the United States Government nor any agency Thereof, nor any of their employees, makes any warranty, express or implied, or assumes any legal liability or responsibility for the accuracy, completeness, or usefulness of any information, apparatus, product, or process disclosed, or represents that its use would not infringe privately owned rights. Reference herein to any specific commercial product, process, or service by trade name, trademark, manufacturer, or otherwise does not necessarily constitute or imply its endorsement, recommendation, or favoring by the United States Government or any agency thereof. The views and opinions of authors expressed herein do not necessarily state or reflect those of the United States Government or any agency thereof.

DISCLAIMER

Portions of this document may be illegible in electronic image products. Images are produced from the best available original document.

ABSTRACT

This project is directed toward establishing an understanding of the relationships between low-stress and gouging wear resistance and microstructure of a series of Ni-Cr white irons and Co-base powder metallurgy (PM) alloys.

The project has been in existence for 24 months, during which time wear testing, optical and quantitative metallography (QTM), and scanning electron microscopy (SEM) have been completed. In this quarterly report, the wear-microstructure interactions of Ni-Cr iron (Ni-Hard 4) samples having various volume fractions of retained austenite are discussed. In addition, the results of detailed SEM studies are considered along with micro-quantitative analyses of the wear scars by energy-dispersive X-ray spectroscopy (EDXS), to provide interpretation of the wear behavior in terms of material removal micro-mechanisms in the white irons.

CONTENTS

1. OBJECTIVE AND SCOPE

The purpose of this research is to develop quantitative relations between microstructure and abrasion resistance of low-to-high Cr white irons (ASTM Series 532) and Co-base powder metallurgy (PM) alloys commonly used in coal conversion processes. The research includes study of gouging wear resistance, necessary in mining operations, and low-stress abrasion resistance, required in coal and coal-product handling and transfer operations. The project has both applied and basic aspects. On the applied side, the establishment of the optimum microstructures for wear resistance is allowing design engineers to make more effective decisions regarding candidate alloys for coal-related processes. From the basic viewpoint, the establishment of a better understanding of the physical and mechanical metallurgy of wear is the foundation for the long-range development of more economical and effective wear-resistant alloys.

The project has been in existence for two years and is currently in a three-month no-cost extension mode, pending action on a two-year renewal proposal. Essentially all of the data acquisition (wear testing, wear scar characterization and microstructure analysis) for the cast irons and PM alloys has been completed and reported in quarterly reports COO-4246-4 through COO-4246-7. In this report the wear data for the cast irons are analyzed in terms of optical metallography, scanning electron microscopy (SEM) and energy-dispersive X-ray spectroscopy (EDXS) studies. This analysis is provided in detail in the Appendix.

2. TASKS AND PROGRESS

2.1 Task I - Preparation of Test Matrix

Task completed 6 June 1977.

2.2 Task II - Preparation of Materials

This task was completed by 15 March 1978, in that by that date all white iron and Co-base alloys had been obtained. The compositions, heat treatments and microstructures of the white irons have been discussed in the quarterly report COO-4246-4, and a similar discussion for the Co-base alloys has been given in quarterly report COO-4246-5.

2.3 Task III - Wear Testing

This task was completed by 15 January 1979, and the test data reported in quarterlies COO-4246-4 through 7. A gouging abrasion wear test system (GAWT), in which a bonded Al_2O_3 abrasive wheel is rotated against the sample, has been used to evaluate gouging wear resistance. A rubber wheel abrasion test system (RWAT) has been used to evaluate low-stress abrasion resistance. In the RWAT procedure, loose SiO_2 or Al_2O_3 abrasive is moved across the sample surface by a rotating steel wheel covered with a chlorobutyl rubber ring. Both tests have been described in detail in quarterly report COO-4246-2 and are summarized in the appendix to this report.

2.4 Task IV - Wear Scar and Microstructure Characterization

This task has been completed and its component sub-tasks have been described in previous quarterly reports as listed below.

2.4.1 Optical metallography of white irons: COO-4246-2.

2.4.2 Optical metallography of Ni-Hard 4 irons of varying retained austenite content: COO-4246-3.

2.4.3 Microtopography of Ni-Hard 4 wear scars: COO-4246-4.

- 2.4.4 Attempted correlation of Ni-Hard 4 wear behavior to mechanical properties: COO-4246-4.
- 2.4.5 Optical metallography, quantitative metallography (QTM) and wear scar microtopography of Co-base PM alloys: COO-4246-5 and COO-4246-6.
- 2.4.6 SEM and EDXS analysis of RWAT and GAWT wear scars of Ni-Hard 4 samples and Co-base PM alloys: COO-4246-7.

2.5 Task IV - Analysis of Data

As was stated previously, Tasks I through IV have been completed, and the task of analyzing and interpreting the experimental data remains. In this quarterly, emphasis is placed on interpreting the data obtained on the Ni-Hard 4 series with varying volume fractions of retained austenite. This analysis and interpretation is presented in detail in the Appendix.

3. SUMMARY

The data acquisition phase of this project has been completed. The results of GAWT testing and RWAT testing with SiO_2 and Al_2O_3 have been reported. These results have been complemented by QTM and SEM-EDXS studies of the wear scars. A detailed interpretation of wear-microstructure interactions for one of the major class of materials studied in project (Ni-Cr white iron) is presented in the Appendix to this report.

4. PERSONNEL

The co-principal investigators, Dr. N. F. Fiore and Dr. T. H. Kosel have devoted 20% and 10% effort respectively during this quarter. Two graduate research assistants, Mr. W. Konkel and Mr. J. Fulcher have devoted 50% and 25% respectively.

COO-4246-8

APPENDIX

ABRASIVE WEAR - MICROSTRUCTURE INTERACTIONS

IN A Ni-Cr WHITE IRON

by

Nicholas F. Fiore, Joseph P. Coyle, Stephen P. Udvardy,

Thomas H. Kosel and William H. Konkel

April 15, 1979

ABRASIVE WEAR-MICROSTRUCTURE INTERACTIONS

IN A Ni-Cr WHITE IRON

by

Nicholas F. Fiore, Joseph P. Coyle, Stephen P. Udvardy,

Thomas H. Kosel and William H. Konkel

Department of Metallurgical Engineering
and Materials Science
University of Notre Dame
Notre Dame, IN 46556

ABSTRACT

The low-stress and gouging wear behavior of a series of Ni-Cr white iron (Ni Hard 4) samples have been characterized. The samples have been processed to contain 5 to 85 percent retained austenite in their microstructures, so that their Rockwell C hardness ranges from 63 to 47. The low-stress abrasion behavior has been measured with loose SiO_2 and Al_2O_3 abrasives in a rubber wheel test system. The gouging abrasion behavior has been determined in a bonded Al_2O_3 wheel test system. Wear scars have been characterized by scanning electron microscopy, used in conjunction with energy-dispersive X-ray spectroscopy.

Both low-stress and gouging wear behavior were strong functions of test condition and microstructure, and weight losses passed through maxima or minima as volume fraction retained austenite or abrasion condition varied. Carbides controlled wear behavior in the low-stress test against SiO_2 , with their attrition occurring by uniform scratching, preferential chipping at leading edges and cracking-spalling. In low-stress and gouging tests against Al_2O_3 , carbides and matrix underwent attrition by uniform micro-machining. The test results indicated that retained austenite content could be used to optimize wear resistance in a variety of abrasion situations.

INTRODUCTION

Abrasive wear is often separated into three classifications [1]: low-stress, grinding and gouging wear. In low-stress abrasion, material attrition is considered to occur by a scratching action which is assumed to leave the abrasive intact. In grinding wear, stresses are assumed to be large enough that the crushing strength of the abrasive is exceeded, so that fresh cutting surfaces are continuously generated. In gouging wear, the abrasive is assumed to rigidly plow through the material, often under impact conditions.

Ni-Cr white irons of the ASTM 532 classification display a number of advantages in these abrasive wear applications. They contain moderate amounts of Ni and Cr, yet they solidify to produce massive Cr-rich carbides in an alloy matrix of sufficient hardenability to be transformed to martensite with relatively simple heat treatment. They show excellent resistance to high-stress grinding abrasion and very good resistance to low-stress scratching abrasion. In addition, because they contain up to 10 w/o Ni and Cr, they retain abrasion resistance in aggressive chemical environments.

On the other hand, in gouging wear or other applications involving moderate to high impact, they perform less satisfactorily. This may be because the large carbides and the martensitic matrix (even when tempered) undergo cracking and spalling in addition to abrasion. Since the irons are C-rich and highly alloyed, their impact resistance may possibly be improved by heat treatment in which retained austenite (γ) is made to co-exist with the more brittle phases.

There is conflicting evidence as to the effect of γ on wear resistance. Zum-Gahr [2] has studied the abrasion resistance of a MnCrV tool steel as a function of retained γ . He employed tests in which pin-like steel samples were abraded against 70 μm Al_2O_3 abrasive disks. The results of his tests,

which probably simulate high-stress abrasion or grinding rather than gouging abrasion with impact, indicate that a minimum in wear tendency exists at intermediate retained austenite content (Table I). In addition, Zum-Gahr found that in this austenite of relatively low alloy content, the abrasive particles induced transformation to martensite. He postulated that at the high γ level near the wear minimum, the martensite formed by the wear process imparted hardness to the matrix and generated compressive stresses which retarded the formation of the microcracks responsible for gross material attrition.

The existence of a minimum in wear tendency may account for some of the ambiguity that exists relative to the role of retained γ , in that wear might increase or decrease with γ volume fraction depending on the range of retained γ used in a particular study. Further evidence of the complexity of the relation between retained γ and wear is provided by the work of Grundlach and Parks [3] on alloy white irons. They employed the high-stress AMAX pin test (APT) in which a pin-like sample traversed back-and-forth against a bonded abrasive paper fixed to the bed of a milling machine [4]. This test probably simulates grinding wear. The irons were of a variety of compositions and were subjected to a number of heat treatments, so that matrices high in γ , martensite or bainite-like γ decomposition products were developed. Moreover, the authors employed SiC (Knoop hardness 2600 HK), Al_2O_3 (2000 HK) and garnet (1400 HK) abrasive papers, so that the effect of abrasive hardness as well as matrix microstructure could be investigated. They found that irons with a bainite-like matrix exhibited poorest wear resistance against all three abrasives. Against SiC and Al_2O_3 , irons with retained γ were superior to martensitic irons, whereas against the softer garnet abrasive the martensitic irons were superior.

Table I

Effect of Retained Austenite on Relative Wear Tendency
of a Hardened MnCrV Tool Steel [2]

% Retained Austenite	Relative Wear Tendency
29	1.12
28	1.02
27	1.00
26	1.02
16	1.00
6	1.22
3	1.34

EXPERIMENTAL

Materials

The abrasion study has been conducted on a Ni-Cr white iron of relatively high alloy content (nominally 6 w/o Ni, 9 w/o Cr). The alloy, whose chemical analysis is given in Table II, falls into the ASTM 532-Type I category and has the designation Ni-Hard 4. It was melted, sand-cast, and then heat treated* according to the schedules listed in Table II to develop retained γ contents of 5%, 20%, 40% and 85%. Retained γ volume fractions were established by point-count on transmission electron micrographs. The melting, heat treatment and quantitative metallographic procedures have been described elsewhere [5].

Following heat treatment, wear samples were cut from the cast blocks on an abrasive-wheel cut-off machine in which the block was completely submerged in coolant. Then they were surface ground (50-90 μm rms roughness) to their final dimensions, with the grinding parallel to the wear direction.

Metallographic samples were prepared from the wear blocks by means of standard procedures. In addition, each wear scar was examined by optical and scanning electron microscopy (SEM). Carbides and other features on the wear scars were subjected to micro-quantitative analysis by means of an energy-dispersive x-ray spectroscopy (EDXS) system interfaced to the SEM.

Low-Stress Abrasion Testing

The low-stress tests have been conducted on a rubber wheel abrasion tester (RWAT) of the type described in ASTM STP 615 [6]. In this test, the sample, in the form of a rectangular parallelepiped, is pressed against a rotating wheel covered with a chlorobutyl rubber ring (Figure 1). An abrasive is fed between the sample and the wheel, and abrasion is characterized by

* Climax Molybdenum Research Laboratories, Ann Arbor, MI 48105

Table II
Characteristics of Ni-Cr White Iron (Ni-Hard 4)

<u>Composition (w/o)</u>								
<u>C</u>	<u>Mn</u>	<u>Si</u>	<u>Cr</u>	<u>Mo</u>	<u>Ni</u>	<u>S</u>	<u>P</u>	<u>N</u>
3.22	.55	1.77	8.9	.04	5.86	.025	.032	.026

Heat Treatment of As-cast Blocks

5% γ - 750°C for 8 h, cooled to -195°C, 210°C for 1 h.

20% γ - 550°C for 4 h, 450°C for 16 h, cooled to -195°C, 210°C for 1 h.

40% γ - 750°C for 8 h, 550°C for 4 h, 450°C for 16 h.

85% γ - 230°C for 4 h.

the weight of loss of the sample.

The wheel consists of a 203 mm diameter steel hub onto which is bonded a 12.7 mm x 12.7 mm chlorobutyl rubber rim. The wheel is rotated at 200 rpm, which corresponds to a linear velocity of 2.38 m/sec. A 13.6 kg mass is applied to a lever system to develop a 0.41 MPa nominal stress to press the sample against the wheel. The white iron samples are 12.7 mm thick x 25.4 mm wide x 76.2 mm long, a length sufficient to contain the entire wear scar.

The abrasive is gravity-fed between the rotating wheel and the sample through a nozzle with a 12.7 mm x 1.6 mm opening. The flow rate of 130 g/mm is maintained for 1000 revolutions, and wear recorded as sample weight loss. The two types of abrasives depicted in Figure 2 have been used: a -50 + 70 mesh semi-rounded Ottawa silica sand^{*}, and an angular Al_2O_3 [†] (nominally 70 mesh).

Gouging Wear Testing

In low-stress wear, the abrasive may relax away from the target surface; however, in gouging wear it is rigidly supported as it plows through the target material. To simulate this situation, Avery and co-workers developed [7] a gouging abrasive wheel tester (GAWT), in which a 254 mm diameter, 70 mesh bonded Al_2O_3 wheel^{**} is rotated at 27 rpm against two samples (wear blocks) which are diametrically opposed (Figure 3). Each sample is held in a lever arm onto which a force of 34.3 N is applied, so that a nominal stress of 0.127 MPa presses the sample to the wheel. One block is 1020 hot-rolled steel, the standard reference material for the GAWT, and the other is the white iron sample.

Before the wear measurement is made, the blocks (originally 11.7 mm x 17.2 mm x 25.4 mm) are "run in" so that cylindrical concave wear surfaces which

^{*} American Foundryman's Society AFS 50-70, Ottawa Silica, Ottawa, IL 61350

[†] Bendix Corporation, Abrasives Division, Marshall, MI 49068.

^{**} Type AR-51177 - Bendix Abrasives, Jackson, MI 49203.

completely conform to the wheel are formed. The actual wear test proceeds in two steps. The number of revolutions necessary to allow 366 m of abrasive to pass each block is set on a decremental counter, and the first phase is run. The two wear blocks are weighed and then interchanged in the arms, so that systematic errors are cancelled. The test is repeated and the blocks weighed again. Gouging wear is characterized either by the weight loss of the sample or by the Abrasion Factor (AF), which is the ratio of the weight loss of the sample to that of the 1020 standard.

The two-step test compensates for slight differences in the wearing action of the two arms. In addition, it provides a built-in check of the validity of each test. Since a 1020 standard is run for all tests, an abnormal weight loss by the standard in either part of the test invalidates the entire test. Under these particular test conditions, the mean weight loss for the 1020 standard is about 1.0 gm, with standard deviation σ of about 0.12 gm. A weight loss outside $\pm 2\sigma$ limits invalidates a test.

RESULTS

Optical Metallography

The microstructures of the Ni-Hard 4 samples of 5, 20, 40 and 85 volume percent retained austenite are displayed in Figure 4. Approximately one-half of the structure is composed of the angular M_7C_3 phase (~ 1700 HK), and the remainder is retained γ and the γ decomposition product. The micrographs show clearly that retained γ is not easily identified optically since it is dispersed within other microstructural constituents. This underscores the necessity of conducting the quantitative electron microscopy.

Wear Testing

The results of the low-stress RWAT abrasion tests with SiO_2 and Al_2O_3 and the gouging test are summarized in Figure 5. Included in the figure are APT results obtained at the Climax laboratories on Al_2O_3 and garnet papers. The plots show wear vs Rockwell C (R_c) hardness, so that percent retained γ decreases toward the right. The data are plotted against hardness because this parameter is assumed to be dominant in theories of abrasive wear [8]. Wear rates inversely proportional to hardness would appear as hyperbolas on such a plot.

The RWAT results with SiO_2 closely coincide with the APT results with garnet, an abrasive of similar hardness. A maximum in wear occurs at 40 volume percent retained γ . The APT results with Al_2O_3 fit this trend, although, as expected, greater weight loss occurs with this harder abrasive. In contrast, the RWAT results with Al_2O_3 show weight loss to monotonically increase as retained γ decreases, in general agreement with the APT results of Grundlach and Parks.

The GAWT results, obtained with the Al_2O_3 grinding wheel, show a minimum rather than a maximum at the intermediate retained γ level. They bear closer resemblance to the results of Zum-Gahr and the RWAT Al_2O_3 data than to the APT

results or the RWAT SiO_2 data.

The data illustrate the extreme sensitivity of wear behavior to microstructure and test conditions. In no case does wear monotonically decrease with increasing hardness, as predicted by theory [8]. The RWAT results with Al_2O_3 are more similar to the GAWT results than to the RWAT results with SiO_2 . In some cases (APT Al_2O_3 , APT garnet, RWAT SiO_2), there is general agreement in wear behavior between various tests, and in other cases, these same tests (APT Al_2O_3 , RWAT Al_2O_3) show opposite behavior. The SEM studies aid in clarifying this complex set of microstructure-test-abrasive interrelationships.

SEM-EDXS Results

In the RWAT test against SiO_2 , sample weight loss varied by about a factor of 1.5, with maximum weight loss occurring at 40% retained γ . This large range in wear resistance is not reflected in the wear scar topography, which is almost identical for the four microstructures. Figures 6a and 6b show the worn surfaces midway down the wear scars of the 5% and the 40% retained γ samples. Both surfaces contain islands which stand out in relief and which are surrounded by regions grooved parallel to wear direction (from right to left). EDXS Cr maps of the surfaces (Figures 6c, 6d) indicate that the islands are the hard, Cr-rich carbides. Although the retained γ content of the matrices varies by a factor of 8, the extent of matrix abrasion in the two samples appears to be identical.

Cracks appear across the carbides in both samples, and craters also appear adjacent to them. Evidently carbides sometimes fracture during the ostensibly "low-stress" wear process and pull out of the surface in the form of discrete fragments. In addition, the abrasive entrance side (right edge) of the carbides shows scratches and scarring, which indicates that the carbides are often removed by gradually being chipped away, rather than by gross fracture.

The role of the carbide phase in imparting wear resistance against SiO_2

for each microstructural state is illustrated in Figure 6a, b. Deep wear grooves traverse the matrix, disappear (or at least become significantly narrower) as they cross the hard carbides, and then appear again in the matrix. Apparently the SiO_2 abrasive particles can cut the matrix of even the 5% retained γ sample with relative ease, but are not effective in scoring the carbides. The preferential wear of the matrix results in the carbides standing out in relief. Carbide attrition appears to take place both by cutting at the leading edges where the matrix has been removed, and by the cracking-fragmentation process previously noted.

Although there are no discernable differences in the central regions of the wear scars of the various SiO_2 RWAT samples, there is a marked difference between the abrasive entrance region and the central region of the scar of any given sample. As is indicated in Figure 7a,b carbides stand out in relief in both regions, but in the entrance region, matrix wear is characterized by short grooves inclined at acute angles to the wear direction. There is evidence that the matrix has been gouged by the abrasive particles and, at points, smeared over the carbides. Evidently in the entrance region the SiO_2 particles have a certain randomness to their motion and are not behaving as simple micro-cutting tools moving rectilinearly.

The sample weight losses in the RWAT tests with the hard Al_2O_3 abrasive were greater by a factor of 5 than those with the SiO_2 abrasive. Moreover the weight loss increased monotonically with hardness, rather than passing through a maximum. SEM analysis of the wear surfaces showed them to be so markedly different from the SiO_2 - worn surfaces, that the differences in wear behavior were not surprising.

The SEM-EDXS results shown in Figure 8 for the Al_2O_3 RWAT test on a 40% retained γ sample are typical of those for the four microstructural states. As is indicated in Figures 8a,b, deep wear tracks or grooves traverse the entire

region of the scar. There is a very subtle indication that the grooves narrow when they traverse carbide particles, and a correspondingly subtle indication of the carbides standing out in relief. At high magnification (Figure 8b), the relief effect is not discernable, and the SEM micrograph and EDXS Cr dot map (Figure 8d) of the same area clearly indicate that the Al_2O_3 particles are uniformly effective in cutting matrix and carbide. There is no evidence of carbide cracking-fragmentation as appeared in the SiO_2 -worn scars, and material attrition appears to be completely by a micro-machining process.

As with the SiO_2 wear scars, the entrance region differs from the mid-region (Figure 8a,c). Short tracks, often inclined to the wear direction, appear on the surface. The carbides do not stand clearly in relief (compare with Figure 7a,b) but the gouged, smeared-metal appearance similar to the SiO_2 entrance region is evident.

The GAWT weight loss passed through a minimum rather than a maximum at 40% retained γ , in contrast with the RWAT SiO_2 loss. Beyond 40% γ , wear increases steeply with hardness as it did in the RWAT Al_2O_3 case. As with the RWAT SiO_2 and Al_2O_3 surfaces, the GAWT surfaces were identical for all four microstructural states of the alloy in spite of a marked difference in weight losses.

The GAWT surfaces were much more similar to the RWAT Al_2O_3 surfaces than to the RWAT SiO_2 . (Note that the Al_2O_3 wheels were fabricated from the same abrasive used in the RWAT Al_2O_3 test). It is apparent from Figure 9 that very deep grooves traverse the entire wear scar, and there are not even subtle indications of carbides in relief. One component of material attrition appears to be the plowing up of thin ridges of material along the grooves. This material is evidently folded back and broken away by the action of the subsequent particles. Rectangular holes in the scar mark the regions where material has broken away

from the groove. Carbides and matrix are cut uniformly by the abrasive, which also must smear matrix material over the carbide surfaces, since no evidence of the harder phases appear (Compare Figure 9b with its corresponding Cr dot map, Figure 9c).

DISCUSSION

Wear Tests

In the most common model of abrasive wear [8], the abrasive is assumed to consist of angular, non-degradable particles which are much harder than the target material. These particles are assumed to partially penetrate the target under the action of an applied load L and to machine V-grooves into the target surface as they move in the direction of wear. The volume and weight of the wear debris is taken to be equal to the volume and weight of the matter originally contained in the grooves. No provision is made in the theory for matter which might be plastically deformed out of the grooves and retained on the target surfaces, for the loss of portions of hard, second-phase particles which may be broken away from the target by brittle fracture, or for preferential attrition of a soft matrix phase which supports a harder phase. Under the simple conditions postulated in the model, the target material is characterized only by its hardness H , and the target weight loss W is described by the relation

$$W = k_{\text{abr}} \frac{Lx}{H} \quad (1)$$

where x is the total displacement of the particles relative to the target, and k_{abr} is a constant which characterizes the angularity of the abrasive.

In this study the simple inverse H relation was not obeyed in any of the wear tests throughout the entire hardness range of the series of samples (R_c 47 to 64, retained γ 85% to 5%). As is indicated in Table III, the relation was followed qualitatively in certain regimes of hardness for certain tests. The agreement may be simply fortuitous in that in the tests with garnet (1400 HK) and SiO_2 (900 HK), the abrasive was softer than the M_7C_3 particles in the matrix (1700 HK), and so a key condition of the model was not obeyed.

Table III

Regimes of Qualitative Agreement with Abrasive Wear Model

Test	Sample Hardness Range (R_C)	Retained γ Range (%)
GAWT - Al_2O_3	47 - 56	85 - 40
RWAT - SiO_2	57 - 63	40 - 5
APT - Garnet	57 - 63	40 - 5
APT - Al_2O_3	57 - 63	40 - 5

Just as the wear data followed the predictions of the sample model in certain regions, they were in agreement with behavior cited in the literature in other regimes. Both Zum-Gahr and Grundlach and Parks found that against hard abrasives (e.g. Al_2O_3), weight loss decreased as volume fraction retained γ increased within certain ranges. The RWAT results on Al_2O_3 and the GAWT results from 5 to 40% retained γ suggest that γ is a useful microstructural constituent against hard, angular abrasives, or conversely that a hard, brittle target is especially susceptible to attrition by harder, angular abrasives.

Zum-Gahr suggested three reasons that the presence of retained austenite should increase wear resistance. First, he observed stress-induced transformation of the retained austenite to martensite, which would provide a local increase in strength, retarding subsurface crack growth. Secondly, the volume expansion which accompanies this transformation would tend to produce surface compressive stresses which would help prevent crack initiation. Thirdly, the stress-induced martensite would only be formed near the surface, and cracks would not easily penetrate into the ductile subsurface austenite. Unfortunately, these arguments do not suffice to explain the present observation of maxima and minima in the wear rate as a function of retained austenite content.

It should be noted that in Zum-Gahr's experiments the primary carbides were smaller than the observed grooves in the worn surfaces, in distinct contrast to the present case. This difference may account for the limitations of his argument.

SEM-EDXS Studies

Perhaps the most surprising result of these studies is that the general appearance of a wear scar is fixed by the test, not the microstructure of the target. For example, the series of samples ranged in hardness from R_c 47 to R_c 63 and correspondingly in retained γ content from 85 to 5 volume percent. In the

RWAT SiO_2 test the weight losses ranged over a factor of 1.5, yet in a given zone the wear scars of various samples were identical. Exactly the same situation obtained for the RWAT Al_2O_3 and the GAWT scars, where a comparable range in weight loss was observed. It is evident that SEM studies, at least at magnifications approaching 1000X, do not give as sensitive a measure of the material attrition processes operative in these tests as might be desired.

On the other hand, the SEM studies clearly differentiate between the tests. In the GAWT, the abrasives cut the matrix and carbide indiscriminantly. Not only is material lost by micro-machining, but substantial amounts of matter are plowed up above the target surface, to be cut or fractured by subsequent abrasive particles. The rectangular holes in the GAWT wear scar may be sites where delamination has occurred, in a manner similar to that described by Doyle and Turley [9] in a single-phase brass.

In the RWAT SiO_2 tests, there is little evidence of plowing up of matter, and the matrices are abraded by micro-machining to a much greater extent than the carbides. The carbides, which consequently stand out in relief, are abraded away at their leading edges, are cracked, and at times pulled out from the matrix (which has been abraded and can no longer support them adequately) in the form of discrete fragments. The relative importance of these two modes of carbide attrition is not known quantitatively, but since most carbides protruding from the worn surfaces do not show evidence of having lost large fragments, it is concluded that chipping away of material from the leading edges of the carbides is the more important process. The carbide surface relief and fracturing were never observed in the GAWT tests.

The RWAT Al_2O_3 surfaces share features with each of the other tests. The abrasive particles cut matrix and carbide particles to an almost identical extent, although there is some evidence of subtle surface relief. There is no

evidence of the plowing-up effect found in the GAWT surfaces or cratering similar to that observed near carbides in the RWAT SiO_2 tests. The increased wear rate observed for Al_2O_3 versus SiO_2 in the RWAT is most certainly due to both the greater hardness of the abrasive and to its much greater angularity. The increased abrasive hardness resulted in easier penetration of the hard carbides, and the greater angularity would lead to a more positive average rake angle. As discussed by Graham and Baul [10] and by Samuels et al [11], abrasives only remove material from a single phase material by machining a continuous chip when the rake angle is more positive than a critical value. In the present case, such chips would probably terminate at carbide sites, but a more positive rake angle would still be expected to increase the efficiency of material removal.

In the RWAT tests with either abrasive it is obvious that the wear process near the entrance region differs from that at the central region, and the fact that the abrasives in the RWAT behave differently at different positions of the sample complicates the already complicated phenomenon of low-stress abrasion. However, the carbides stand in relief in both the entrance and mid-regions of the SiO_2 RWAT wear scars.

The SEM studies provide valuable insight as to why simple pictures of abrasive wear lead to erroneous conclusions. The material attrition process assumed in the mathematical derivation greatly over-simplifies the actual wear processes. In the GAWT and the RWAT Al_2O_3 tests, the abrasive does act by micro-machining, but the plowing-up, cutting and fracturing of ridges of material protruding above the wear surface is an important aspect of material attrition. This plowing-up is completely neglected in the theory.

Microstructural Features and Wear Resistance

In the case of the SiO_2 RWAT test, the hardness of the carbides (~1700 HK) is greater than that of the abrasive (~900 HK). The carbides are therefore not easily cut by the abrasive, and so they are left protruding from the surface after the surrounding matrix has been worn away (Figures 6,7). Over a substantial portion of the surface (greater than 50%), the carbides are spaced closely enough that the matrix material between them is not removed until the more resistant carbides have been cut or chipped away. In these areas the carbides control the wear resistance. In the remainder of the surface, which consists of large areas of matrix material (Figures 6,7), long straight grooves are formed. Consequently, the factors controlling the wear rate of these different areas of the surface differ, and may interact in such a way that a maximum or minimum in wear may result.

In the GAWT and Al_2O_3 RWAT tests, the carbides do not control the wear rate over a large fraction of the surface. In the GAWT test, the groove depth is the same in the carbides as in the matrix areas, and this is almost true in the case of the Al_2O_3 RWAT. Since the Al_2O_3 abrasive hardness (~2000HK) is greater than that of the carbides (~ 1700 HK), the abrasive should be expected to cut the carbides more effectively than SiO_2 . However, if hardness were the only factor affecting groove depth, the difference in depths in the matrix and carbides would be expected to be greater in the Al_2O_3 RWAT case. This follows since in the GAWT case, the load and penetration depth of any given abrasive particle are largely determined by the distribution of the externally applied load over all contact points between the abrasive wheel and the specimen. Deflection of the abrasive particle by a carbide would require reducing the load carried at all other contact points, so the carbides are necessarily cut through. In contrast, the load on individual abrasive particles in the RWAT case is independently applied by the indentation of

the particle into the rubber wheel, so that the abrasive particle can change its depth of cut when it reaches a carbide.

Factors which may affect the wear rate in the Al_2O_3 RWAT and GAWT tests include the rake angles of the abrasive particles, the critical rake angles of the various microconstituents [9,10], thermal effects on the microstructure, and stress-induced transformation of retained austenite to martensite.

The average rake angle of the Al_2O_3 particles in the RWAT test is probably considerably more positive than that of the SiO_2 abrasive, which would lead to more efficient cutting due to a greater proportion of chip-forming contacts relative to plow-forming contacts as described by Graham and Baul [9] and by Turley and Doyle [10]. Thus the Al_2O_3 abrasive might be expected to cut more efficiently than SiO_2 because of both its angularity and its hardness. The presence of a minimum in wear rate for the 40% retained γ microstructure in the GAWT may reflect a more positive critical rake angle for this structure. However, this effect cannot be separated from the other effects discussed.

In view of the large number of difference in test conditions between the SiO_2 RWAT and the GAWT, the changing effectiveness of the microstructures is not surprising; however, much experimental work would be required to isolate the effects of each variable.

CONCLUSIONS

1. Both low-stress and gouging wear behavior of the Ni-Cr white iron studied are strong functions of its microstructural state, especially the retained γ content of its matrix.
2. In both gouging and low-stress wear against a very hard abrasive (Al_2O_3), matrix and carbide undergo uniform attrition by a micro-machining actions
3. In low-stress wear against SiO_2 , an abrasive of hardness intermediate between matrix and carbide, the material attrition mechanisms are much different than those against Al_2O_3 . The matrix is abraded preferentially by micro-machining, and then the carbides which stand out in relief are chipped away at their exposed leading edges and are to a lesser extent lost by fracture and spalling. The resistance of the carbides to the softer abrasive appears to be mainly responsible for the factor of 5 improvement in wear resistance over the Al_2O_3 case.
4. Over a substantial fraction of the surface, the carbides control the wear rate in the SiO_2 RWAT. This is not true in the GAWT or Al_2O_3 RWAT tests, and the large number of variables present do not permit conclusive evaluation of the factors controlling wear in the latter tests.
5. In the low-stress tests, in which the abrasive has greater freedom than in the gouging, the entrance region shows evidence of a more random direction of particle travel than in the central region. This may be a limitation of the test, in that the abrasive is not behaving uniformly as it moves along the sample surface.
7. SEM-EDXS studies are extremely useful in illustrating differences in material attrition processes in the various tests. They are less effective in differentiation between differences in sample behavior in a given test.

ACKNOWLEDGMENT

This work has been supported by the Division of Fossil Energy, U. S. Department of Energy. The authors are indebted to the staff of this division for their cooperation. In addition, the authors express their appreciation to Mr. Douglas Doane, Mr. William Scholtz and Mr. James Parks of the Climax Research Laboratories for their cooperation in providing the Ni-Hard 4 samples and to Mr. Howard Avery for his essential commentary on the work.

REFERENCES

1. Avery, H. S., "The Nature of Abrasive Wear," SAE Publication 750822, 1-15 (1975).
2. Zum-Gahr, K. H., "The Influence of Thermal Treatments in the Abrasive Wear of Tool Steels," Zeitschrift fur Metallkunde, 68, 783-92 (1977).
3. Grundlach, R. B., and Parks, J. L., "Influence of Abrasive Hardness of Wear Resistance of High Chromium Irons," Wear of Metals (ASME, New York, 1977), p. 211-216.
4. Muscara, J. and Sinnott, M. J., "Construction and Evaluation of a Versatile Abrasive Wear Testing Apparatus," Metals Engineering Quarterly, 12, 21-32 (1972).
5. Diesburg, D. E., "Performance of Competitive Abrasion Resistant Irons in Laboratory Tests, Report L-212-138 (Climax Molybdenum Research Laboratories, Ann Arbor, MI, 1975).
6. Miller, A. E. and Tucker, R. C., Low Stress Abrasive and Adhesive Wear Testing, ASTM STP 615 (ASTM, Philadelphia, 1976).
7. Avery, H. S., Surface Protection Against Wear and Corrosion, (ASM, Metals Park, OH, 1954), p. 24.
8. Rabinowicz, E., Friction and WEar of Materials (Wiley, New York, 1965), p. 168.
9. Graham, D. and Baul, R. M., "An Investigation into the Mode of Metal Removal in the Grinding Process," Wear, 19, 301-314 (1972).
10. Turley, D. M., and Doyle, E. D., "Factors Affecting Workpiece Deformation During Grinding," Mat. Sci. and Engr., 21, 261-271 (1975).
11. L. E. Samuels, "The Mechanisms of Arasive Machining," Scientific American 239, 132-52 (1978).

LIST OF TABLES

Table I. Effect of Retained Austenite on Relative Wear Tendency of a Hardened MnCrV Tool Steel.

Table II. Characteristics of Ni-Cr White Iron (Ni-Hard 4).

Table III. Regimes of Qualitative Agreement with Abrasive Wear Model.

LIST OF FIGURES

Figure 1. Dry-Abrasive Rubber Wheel Abrasion Tester (RWAT).

Figure 2. SEM Micrographs Abrasive Employed in Rubber Wheel Abrasion Tester (60X). a) Semi-rounded Ottawa Silica Sand (AFS 50-70), b) Angular Alumina (70 mesh).

Figure 3. Gouging Abrasion Wear Test (GAWT) Apparatus.

Figure 4. Microstructures of Four Types of Ni-Hard 4 Samples. M_7C_3 Carbides (White) in Matrices of Various Percentages Retained Austenite with Austenite Decomposition Products. a) 5% γ , b) 20% γ , c) 40% γ , d) 85% γ . All are at 900X

Figure 5. RWAT, APT and GAWT Results on Ni-Hard 4 Samples (Percent Retained Austenite Decreases toward the Right).

Figure 6. SEM Micrographs and EDXS Cr Dot Maps of SiO_2 RWAT Ni-Hard 4 Test Samples. a) Central Region of Scar of 5% Retained γ Sample (900X) b) Central Region of Scar of 40% Retained γ Sample (900X), c) Cr Dot Map of 6a, d) Cr Dot Map of 6b.

Figure 7. SEM Micrographs of SiO_2 RWAT Ni-Hard 4 Samples with 5% Retained γ . a) Abrasive Entrance Region (360X), b) Central Region (360X).

Figure 8. SEM Micrographs and EDXS Cr Dot Maps of Al_2O_3 RWAT Ni-Hard 4 Test Samples. a) Central Region of 40% Retained γ Sample (360X), b) Central REgion of 40% Retained γ Sample (900X), c) Entrance Region of 40% Retained γ Samples (360X), d) Cr Dot Map of 8b.

Figure 9. SEM Micrographs and EDXS Cr Dot Maps of GAWT Wear Scars. a) 40% Retained γ (360X), b) 40% Retained γ (900X), c) Cr Dot Map of 9b.

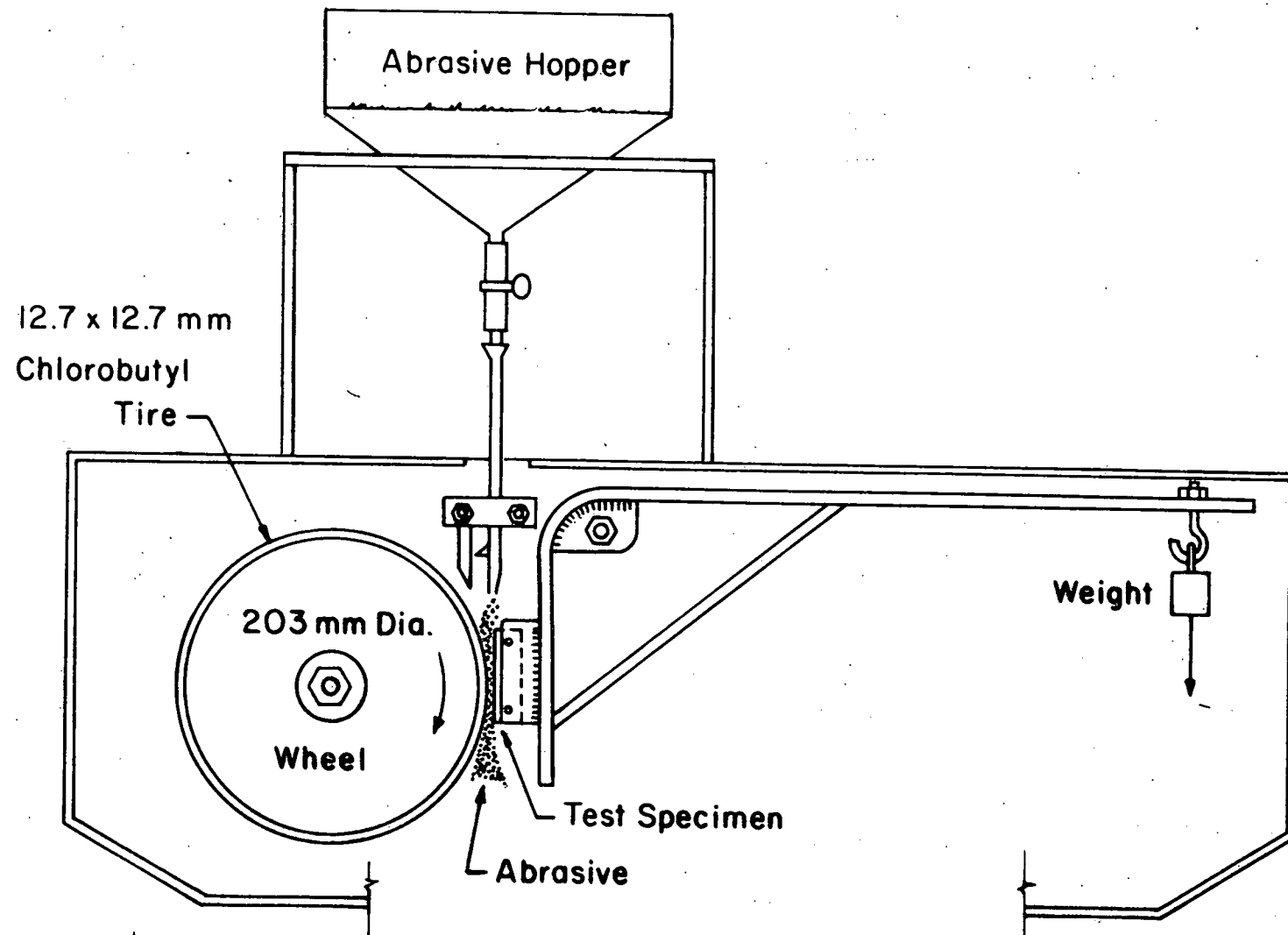


Figure 1. Dry-Abrasive Rubber Wheel Abrasion Tester (RWAT).



a) Semi-Rounded Ottawa Silica Sand (AFS 50-70)



b) Angular Alumina (70 mesh)

Figure 2. SEM Micrographs. Abrasives Employed in Rubber Wheel Abrasion Tester (60X).

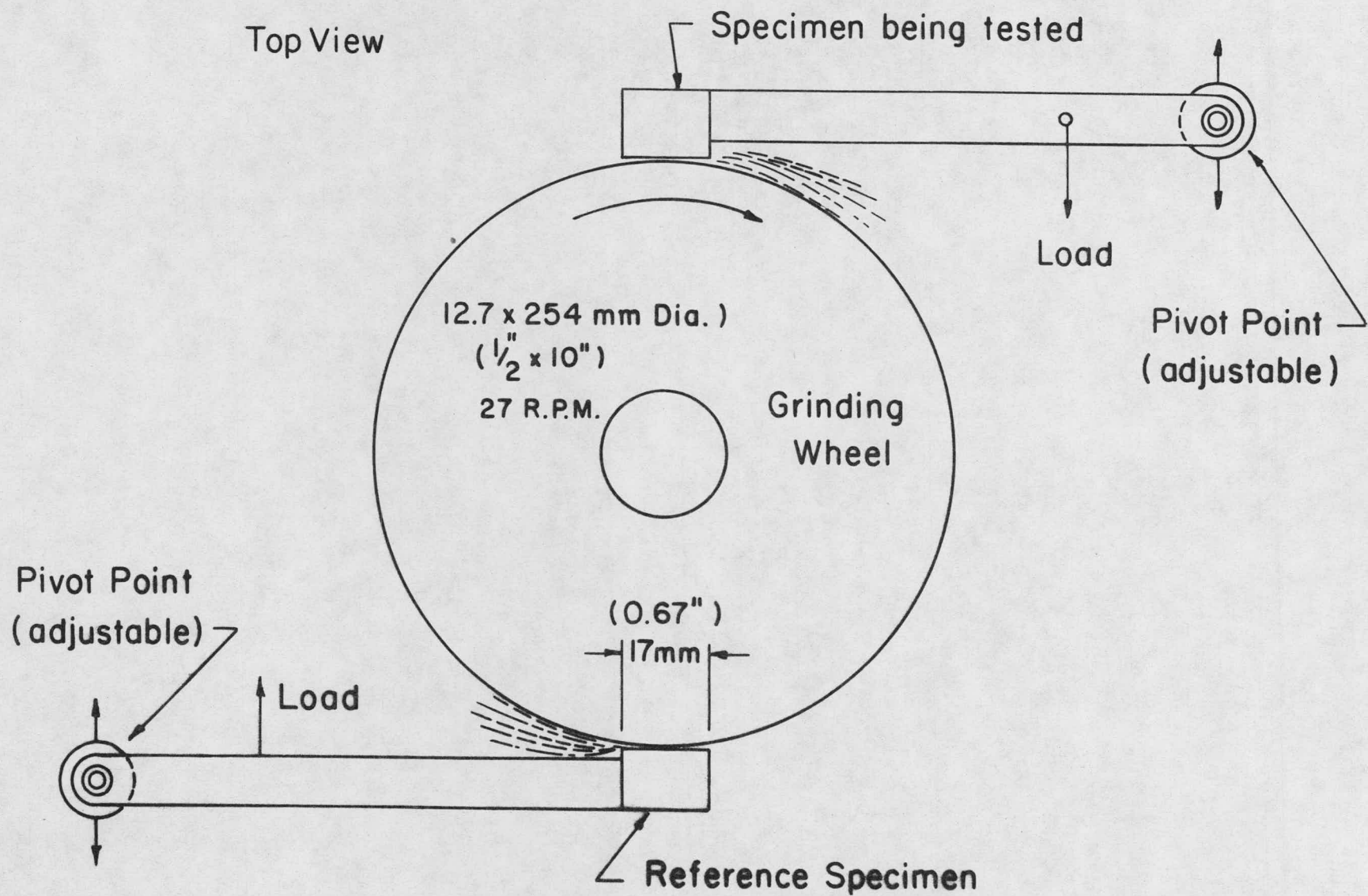
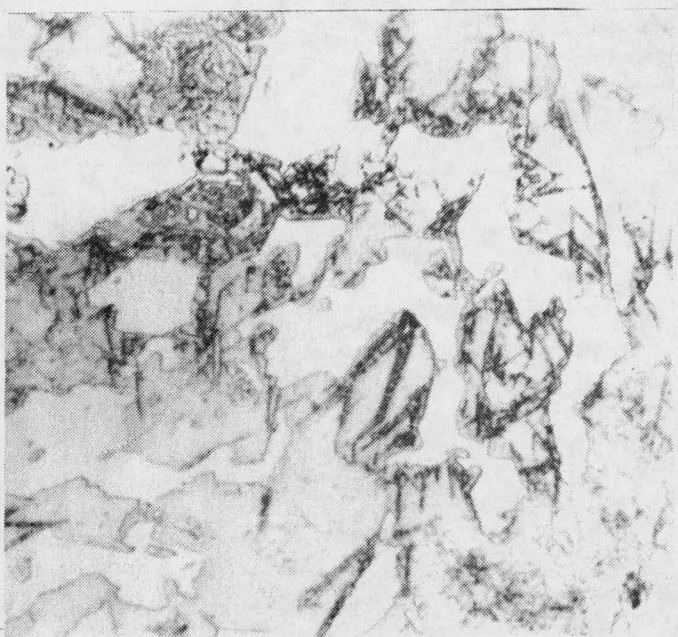


Figure 3. Gouging Abrasion Wear Test (GAWT) Apparatus.



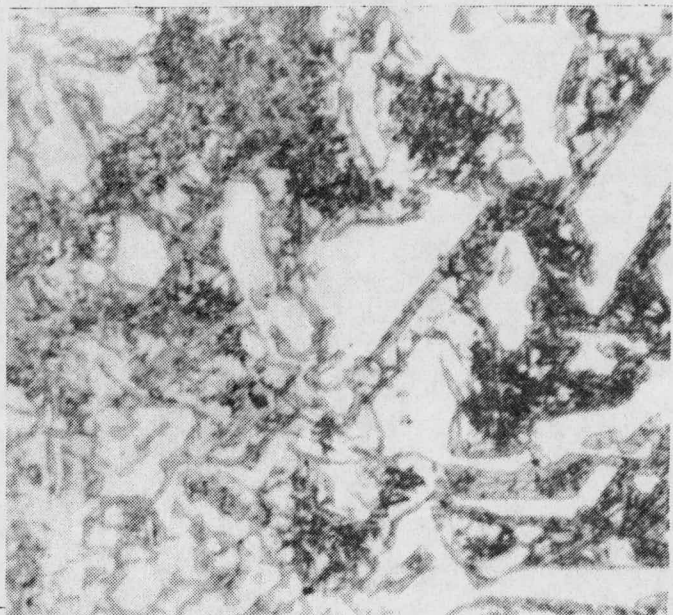
a) 5% Retained γ

(a)



b) 20% Retained γ

(b)



c) 40% Retained γ



d) 85% Retained γ

Figure 4. Microstructures resulting from the four different heat treatments of the Ni-Hard 4 cast iron. M_7C_3 carbides (white) in matrices of various percentages of retained austenite with austenite decomposition products. (a) 5% γ ; (b) 20% γ ; (c) 40% γ ; (d) 85% γ . All are at 900X.

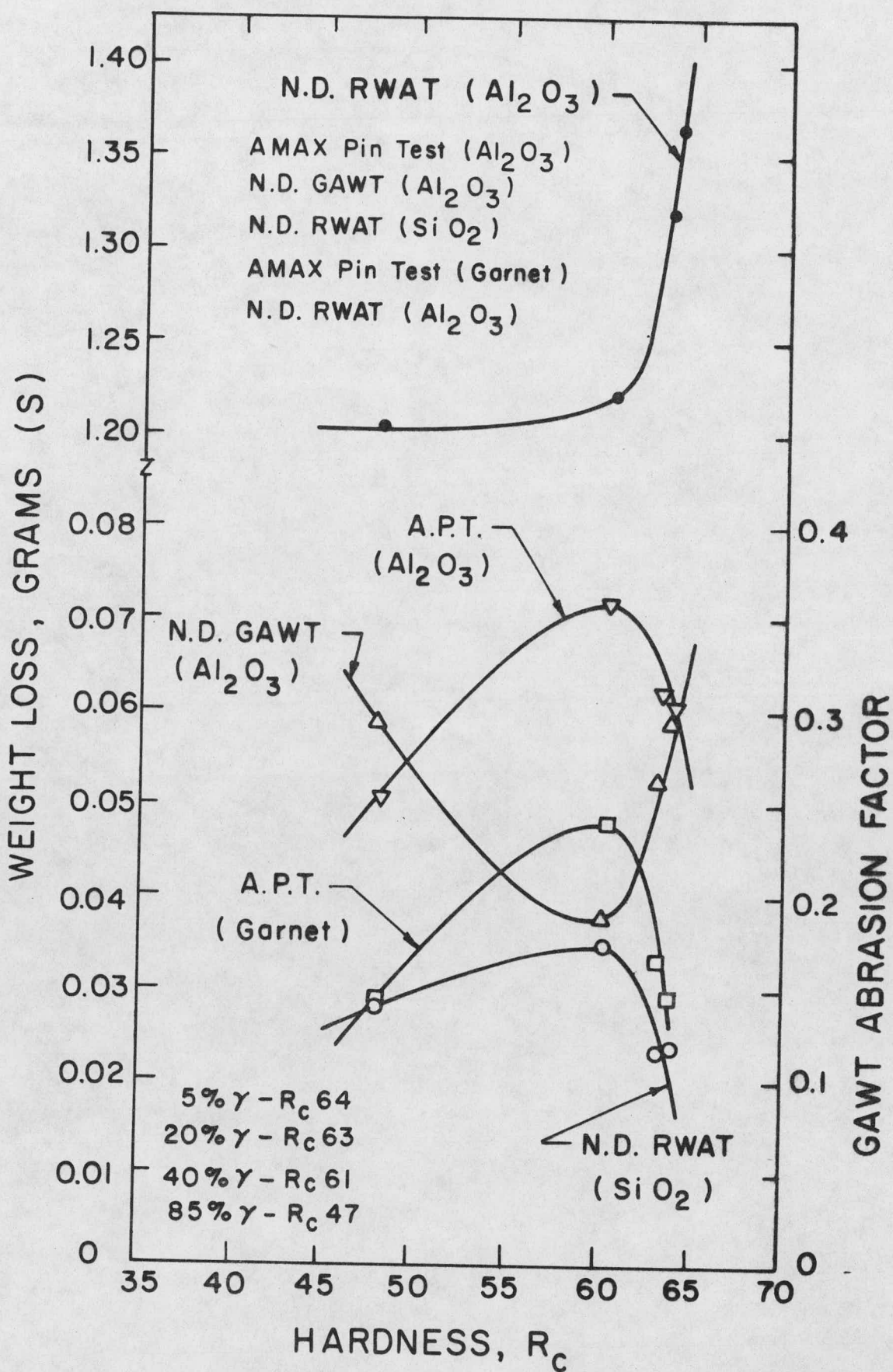
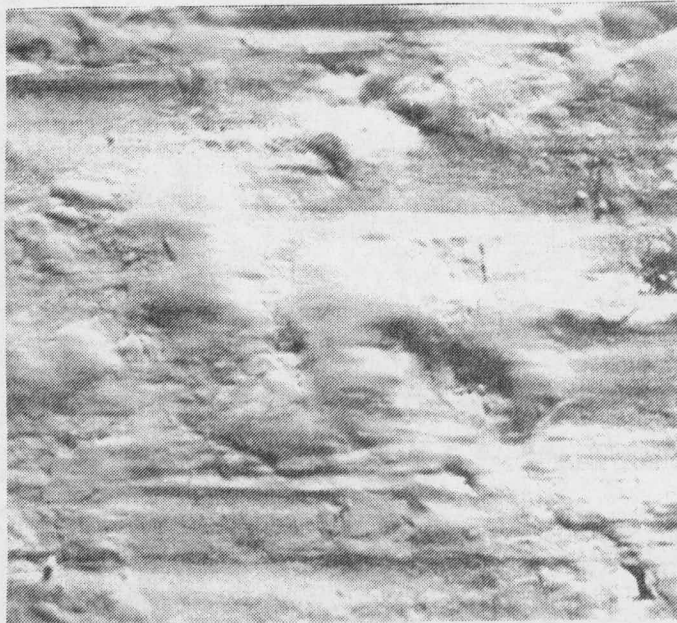
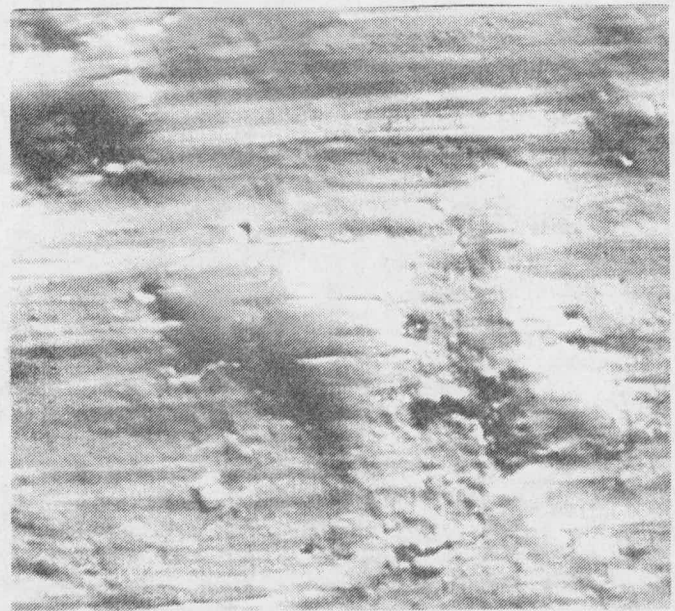


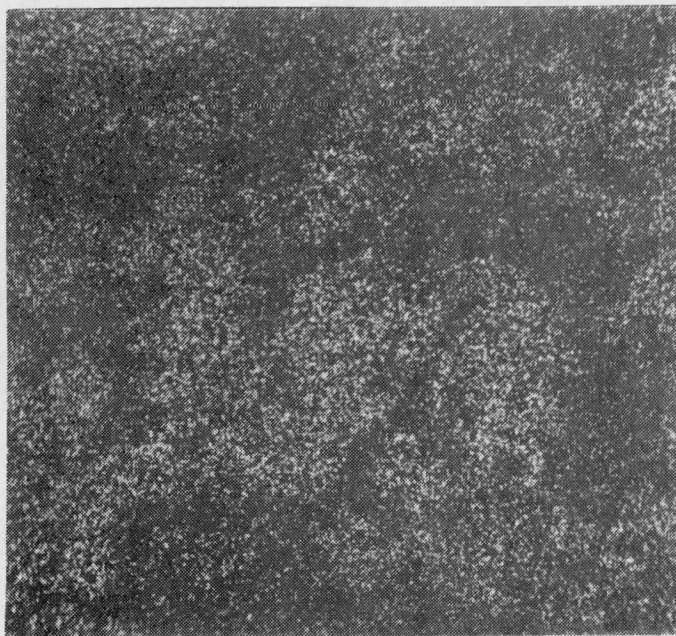
Figure 5. RWAT, APT and GAWT Results on Ni-Hard 4 Samples
(Percent Retained Austenite Decreases toward the Right)



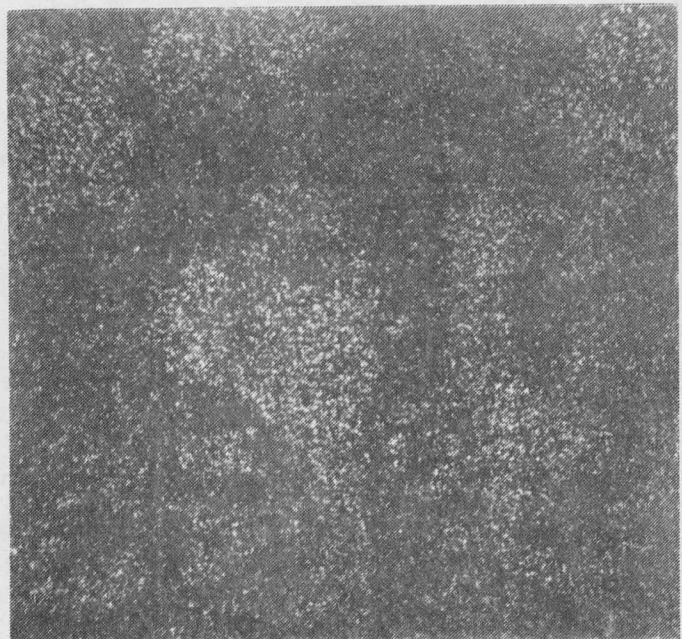
a) Central Region of Scar of 5%
Retained γ Sample (900X)



b) Central REgion of Scar of 40%
Retained γ Sample (900X)



c) Cr Dot Map of 6a.

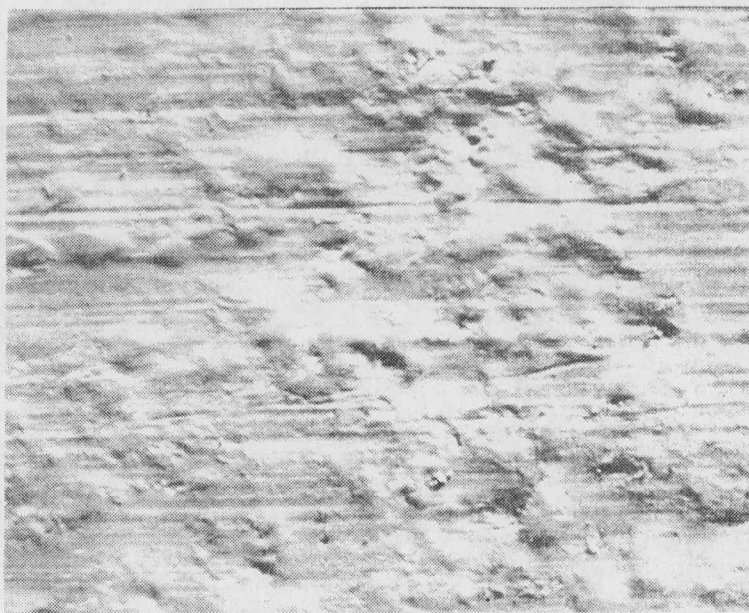


d) Cr Dot Map of 6b.

Figure 6. SEM Micrographs and EDXS Cr Dot Maps of SiO_2 RWAT Ni-Hard 4
Test Samples.



a) Entrance Region (360X)



b) Central Region (360X)

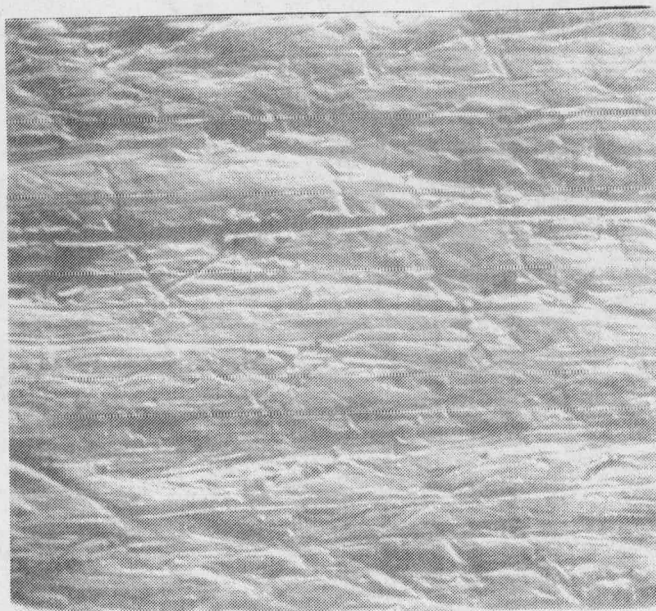
Figure 7. SEM Micrographs of SiO_2 RWAT Ni-Hard 4 Samples with 5% Retained γ .
(a) Abrasive Entrance Region (360X), (b) Central Region (360X).



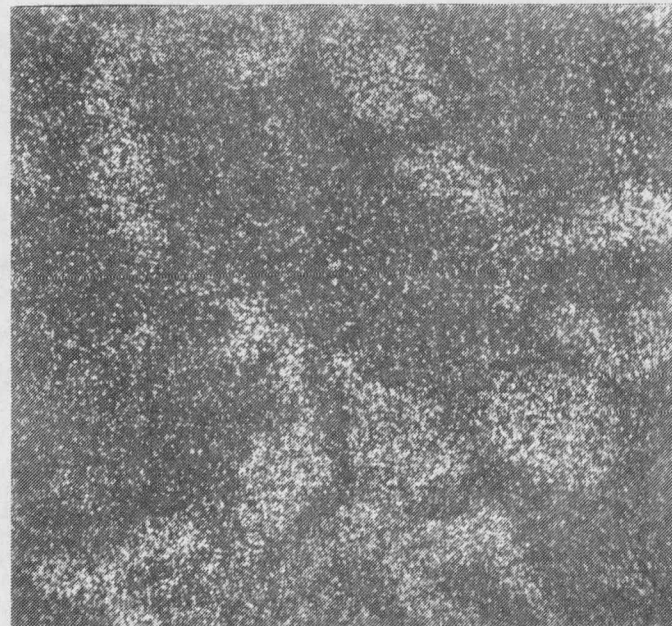
a) Central Region of 40% Retained γ
Sample (360X)



b) Central Region of 40% Retained γ
Sample (900X)



c) Entrance Region of 40% Retained γ
Sample (360X).

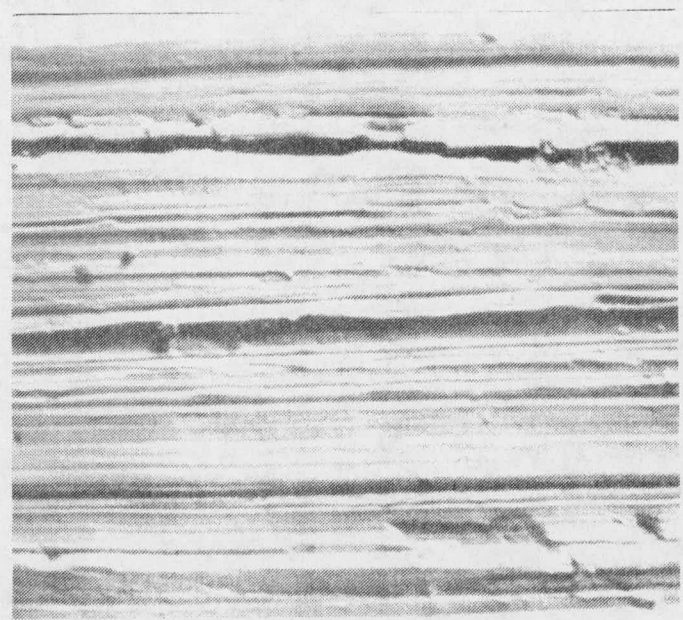


d) Cr Dot Map of 8b.

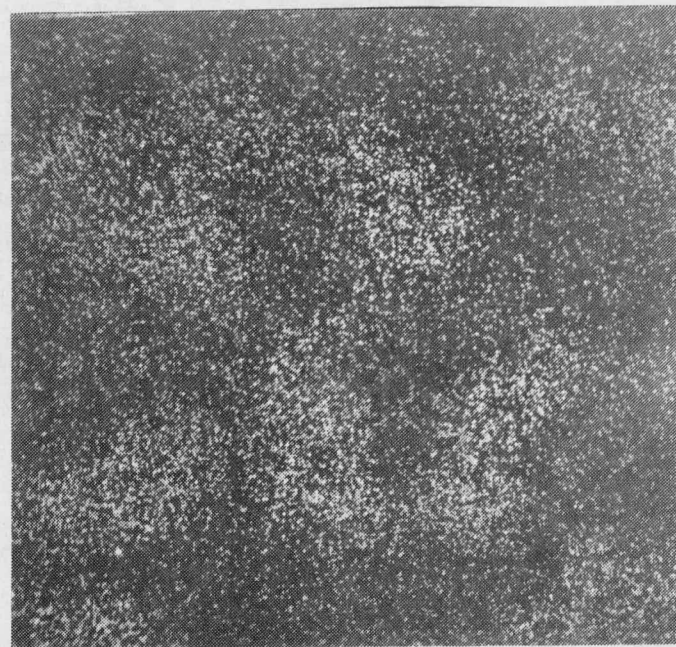
Figure 8. SEM Micrographs and EDXS Cr Dot Maps of Al_2O_3 RWAT Ni-Hard 4
Test Samples.



a) 40% Retained γ (360X)



b) 40% Retained γ (900X)



c) Cr Dot Map of 9b

Figure 9. SEM Micrographs and EDXS Cr Dot Maps of GAWT Wear Scars.

DISTRIBUTION LIST

Mr. John J. Mahoney
Senior Contract Administrator
Contracts Management Office
DOE- Chicago Operations Office
9700 South Cass Avenue
Argonne, IL 60439
- 6 copies -

Dr. S. J. Dapkus
Division of System Engineering/
Energy Technology
U.S. D.O.E.
Room C-155
Germantown, MD 21401
- 3 copies -

Dr. Paul Scott
Division of System Engineering/
Energy Technology
U.S. D.O.E.
Room C-155
Germantown, MD 21401

Dr. Sam Schneider
National Bureau of Standards
Washington, D.C. 20234

Dr. John Dodd
Climax Molybdenum Company
13949 West Colfax Avenue
Golden, CO 80401

Metals and Ceramics Information Center
Battelle-Columbus Laboratories
505 King Avenue
Columbus, OH 43201

Dr. J. L. Parks
Climax Molybdenum Research Lab
1600 Huron Parkway
Ann Arbor, MI 48106

Dr. M. S. Bhat
Materials and Molecular Research Div.
Bldg. 62 - Room 239
Lawrence Berkeley Laboratory
University of California
Berkeley, CA 94720

Mr. Howard Avery
69 Alcott
Mahwah, N.J. 07430

Dr. Kenneth Antony
Stellite Division
Cabot Corporation
Kokomo, IN 46901

Dr. Stanley Wolf
Materials Science Program
Basic Energy Sciences Division
D.O.E.
Washington, D.C. 20545

Dr. Joseph Klein
Stellite Division
Cabot Corporation
Kokomo, IN 46901

Dr. Jerry L. Arnold
Research and Technology
Armco Steel Corporation
Middletown, OH 45043

Dr. R. C. Tucker
Union Carbide Corp.
1500 Polco Street
Indianapolis, IN 46224

Dr. Paul Swanson
Deere and Company Technical Center
3300 River Drive
Moline, IL 61265

Dr. Jeffrey S. Hansen
P.O. Box 70
Bureau of Mines
Albany, OR 97321

Dr. R. J. Dawson
Falconbridge Nickel Mines Ltd.
P.O. Box 900, 8810 Yonge St.
Thornhill, Ontario, Canada L3T 4A8

Dr. Burton R. Patterson
Southern Research Institute
2000 Ninth Avenue, South
Birmingham, AL 35205